Published in final edited form as:

Nat Neurosci. 2016 April ; 19(4): 587–595. doi:10.1038/nn.4263.

Circadian rhythms in neuronal activity propagate through output circuits

Matthieu Cavey[1,2,4], **Ben Collins**[1,5], **Claire Bertet**[1,4], and **Justin Blau**[1,2,3,6]

[1]Department of Biology, New York University, 100 Washington Square East, New York, NY 10003, USA

[2]Center for Genomics & Systems Biology, New York University Abu Dhabi Institute, Abu Dhabi, United Arab Emirates

[3]Program in Biology, New York University Abu Dhabi, Abu Dhabi, United Arab Emirates

Abstract

24hr rhythms in behavior are organized by a network of circadian pacemaker neurons. Rhythmic activity in this network is generated by intrinsic rhythms in clock neuron physiology and communication between clock neurons. However, it is poorly understood how the activity of a small number of pacemaker neurons is translated into rhythmic behavior of the whole animal. To understand this, we screened for signals that could identify circadian output circuits in *Drosophila*. We found that Leucokinin neuropeptide (LK) and its receptor (LK-R) are required for normal behavioral rhythms. This LK/LK-R circuit connects pacemaker neurons to brain areas that regulate locomotor activity and sleep. Our experiments revealed that pacemaker neurons impose rhythmic activity and excitability on LK and LK-R expressing neurons. We also found pacemaker neuron-dependent activity rhythms in DH44-expressing neurons, a second circadian output pathway. We conclude that rhythmic clock neuron activity propagates to multiple downstream circuits to orchestrate behavioral rhythms.

INTRODUCTION

Innate behaviors such as circadian rhythms are hardwired into the nervous system, making them particularly useful to study how information flows through neuronal circuits to generate behavior. Circadian rhythms in behavior help animals anticipate predictable daily

[6]Corresponding author: justin.blau@nyu.edu.

[4]Current address: Aix-Marseille Université, CNRS, IBDM UMR7288, 13009 Marseille, France

[5]Current address: Institute of Pharmacology and Toxicology, University of Zürich, Winterthurerstrasse 190, 8057 Zürich, Switzerland

AUTHOR CONTRIBUTIONS

MC and BC performed the RNAi screen. MC performed all other experiments and analyses except immunostaining in Supplementary Figure 3 by CB. MC and JB wrote the manuscript, with comments from BC and CB.

COMPETING FINANCIAL INTERESTS

The authors declare no competing financial interests

Code availability

All IgorPro scripts are available upon request.

A supplementary methods checklist is available.

changes in the environment [1, 2] and are controlled by circadian pacemaker neurons. These neurons contain molecular clocks that drive rhythmic gene expression and set up 24hr rhythms in pacemaker neuron resting membrane potential, spontaneous firing rate and overall excitability [3]. Communication between clock neurons synchronizes their molecular clocks and adds robustness to the system [2]. Specific subgroups of clock neurons have peak neuronal activity at different times of day from each other and presumably regulate distinct output circuits to drive numerous rhythmic behaviors including locomotor activity, sleep and feeding [1]. However, how the clock neuronal network controls different output circuits remains poorly understood.

Rhythms in pacemaker neurons could propagate to downstream cells via two mechanisms. Clock neurons can act on distant cells via rhythmic hormonal signals which entrain and synchronize molecular clocks in peripheral tissues. For example, clock neurons control rhythmic glucocorticoid release from the adrenal gland into the bloodstream, which then helps reset the molecular clocks in peripheral organs such as the liver [4]. Clock neurons could also impose rhythmic activity on downstream neurons via direct neuronal communication. Although many neurons fire rhythmically in the mammalian brain, widespread clock gene expression in mammals makes it difficult to exclude a role for local clocks in these rhythms [5].

Studies of *Drosophila* have been instrumental in dissecting the molecular and neuronal bases of circadian rhythms [2]. However, how clock outputs are mediated in *Drosophila* remains poorly understood. Although peripheral clocks control rhythms in eclosion [6] and feeding [7], the clock output circuits controlling locomotor activity rhythms and sleep remain elusive. These outputs probably converge on the Central Complex (CC) [8], Pars Intercerebralis (PI) [9, 10] and the Mushroom Bodies [11-13]. One output pathway links the small LN_v principal pacemaker neurons (s-LN_v) to DN_{1p} clock neurons, which then innervate a subset of PI neurons that express the DH44 neuropeptide. These DH44-expressing neurons are required for circadian rhythms [10], but how their activity is regulated by the clock network has not been addressed. A second likely clock output pathway involves CC neurons that respond to Pigment Dispersing Factor (PDF) released from LN_vs, although the role of these CC neurons in circadian behavior has not yet been determined [14]. A third output pathway involves DH31 release from DN_1 clock neurons to regulate sleep, but the relevant targets remain to be characterized [15].

Here, we identified an additional circadian output circuit connecting clock neurons to locomotor and sleep centers in the brain. This circuit comprises a pair of non-clock neurons expressing the neuropeptide Leucokinin (LK) and a set of downstream neurons expressing the Leucokinin Receptor (LK-R) that project to the CC. Using calcium imaging, we demonstrate that clock neurons impose 24hr rhythms on the excitability and activity of LK and LK-R neurons by neuronal communication. We also show that LK and LK-R neurons control the rhythmicity and levels of locomotor activity and sleep. In addition, we found that clock neurons also impose activity rhythms on the previously characterized DH44 circadian output neurons. Thus propagation of clock neuron electrical rhythms is a general mechanism for organizing circadian rhythms of behavior via multiple circuits.

RESULTS

Leucokinin signaling is required for circadian rhythms

We hypothesized that we could identify a novel circadian output circuit by screening for circadian behavioral defects in flies mutant for a signaling molecule and/or its relevant receptor. We chose neuropeptides since they usually have more restricted distributions than neurotransmitters and since many neuropeptides modulate neuronal activity to regulate specific behaviors, such as PDF in circadian rhythms [16, 17].

We used transgenic RNAi lines expressed via the pan-neuronal driver *elav-Gal4* to knockdown *Drosophila* neuropeptides in the whole brain and then assayed adult locomotor rhythms in constant darkness (DD; **Fig. 1a** and **Supplementary Table 1**). We found 4 RNAi transgenes that significantly weakened behavioral rhythms: *Bursicon*, *SIFamide, Leucokinin* (*Lk*) and *Nplp3* (**Fig. 1a-b**). We focused on *Lk* because it does not seem to be involved in development and has an intriguing expression pattern in the brain (see below).

To further test a role for *Lk* signaling in circadian rhythms, we used RNAi to knockdown the *Leucokinin Receptor* (*Lkr)*. This also weakened behavioral rhythms (**Fig. 1b** and **Supplementary Table 2**). To complement these RNAi experiments, we assayed the behavior of Lk^{c275} and Lkr^{c003} hypomorphic flies, which have reduced LK peptide and LK-R protein levels [18]. These mutants had weaker rhythms than heterozygous control flies. Lkr^{c003} and additional *Lkr* alleles gave similar behavioral phenotypes as hemizygotes (**Fig. 1c-d, Supplementary Fig. 1a** and **Supplementary Table 2**).

Quantifying LK peptide levels and *Lkr* RNA in the different mutants revealed that the strength of behavioral phenotypes correlates with the extent of knockdown: LK levels are reduced much more strongly by Lk^{RNAi} than Lk^{c275}, with only 3% of wild type LK levels in Lk^{RNAi} flies and stronger effects on behavior than for Lk^{c275} (**Supplementary Fig. 1b-c** and **Supplementary Table 2**). *Lkr* RNA levels are reduced to similar levels in Lkr^{c003} hypomorphs and Lkr^{RNAi} knockdowns (**Supplementary Fig. 1d**) and have similar strength behavioral phenotypes (**Supplementary Table 2**).

Together, these RNAi and mutant analyses indicate that LK signaling is important in adult circadian rhythms. We have not been able to test a specific role for *Lk* in adult neurons since restricting Lk^{RNAi} expression to adulthood did not reduce LK peptide levels (data not shown). Below we describe how manipulating the activity of LK and LK-R expressing neurons in adults alters rhythmic locomotor activity.

LK and LK-R neurons are not clock neurons

Next we tested if LK and LK-R neurons are clock neurons themselves. LK is expressed in only 4 neurons in the adult brain [19]: one pair of neurons (SELKs) in the Sub-Oesophageal Ganglion (SOG) and another pair in the Lateral Horn, the Lateral Horn LK neurons (LHLKs; **Fig. 1e**). Since the DN_3 group of clock neurons is close to LHLK cell bodies, we examined LK staining with clock neuron markers. We found that LHLK neurons do not produce the essential clock protein TIMELESS (TIM, **Fig. 1f**) nor do they express *tim*- or *per-Gal4* (**Fig. 1g** and **Supplementary Fig. 2a**). We also expressed a dominant negative

cycle transgene (*UAS-cycΔ* [20]) to block the molecular clock. *UAS-cycΔ* completely abolished behavioral rhythms when expressed in clock neurons via *tim-Gal4*, but had no effect when expressed in LK neurons (**Supplementary Fig. 2b** and **Supplementary Table 2**).

To examine *Lkr* expression, we used an *Lkr-Gal4* line that recapitulates endogenous LK-R expression [18]. *Lkr* is more widely expressed in the brain than LK and is also present in regions where clock neurons are located (**Fig. 1h**). However, we could not detect TIM expression in *Lkr-Gal4* expressing neurons (**Fig. 1i**) and locomotor rhythms were unaffected by expressing *UAS-cycΔ* in LK-R neurons (**Supplementary Fig. 2b** and **Supplementary Table 2**). Thus we conclude that LK and LK-R neurons are not clock neurons.

Finally, we tested whether LK signaling affects the molecular clock in pacemaker neurons. We measured TIM and VRI oscillations in the strong Lk^{RNAi} knockdown on the second and third days in DD and found that rhythms were very similar to control flies (**Supplementary Fig. 2c-e**). Thus LK signaling is likely downstream of the clock since Lk^{RNAi} disrupts behavior without affecting molecular clock rhythms.

LHLK neurons project close to clock neurons

To test if LK and LK-R neurons are outputs of the clock, we wanted to determine if they communicate with clock neurons. We first analyzed their anatomy and found that LHLK projections (marked by LK staining) are very close to the dorsal projections of the s-LN_v clock neurons (**Fig. 2a**). To more clearly visualize LHLK projections, we used an *Lk-Gal4* line that recapitulates endogenous LK expression [19] and the GFP amplification cassette FLEXAMP [21]. This revealed numerous sites of potential contact between s-LN_v and LHLK projections (**Fig. 2a**, inset). Several clock neuron classes converge at the s-LN_v dorsal projections [22] and we also found LK staining very close to projections of DN_{1p} and LN_d clock neurons (**Fig. 2b,c**). These data are consistent with LHLKs communicating with one or more classes of clock neurons.

Next we examined the location of LK neuron synaptic and dendritic markers. We expressed DenMark [23] and Syt::GFP [24] in LHLK neurons to simultaneously label LHLK input and output areas respectively and used PDF to label the clock network output region. We found that DenMark accumulates in LHLK neurons close to s-LN_v projections with LHLK dendrites often intermingling with s-LN_v projections in single confocal sections (**Fig. 2d-e**). In contrast, we mainly found Syt::GFP in more posterior sections of LHLK neurons, which do not contain s-LN_v projections (**Fig. 2d**). Since s-LN_vs have pre-synaptic markers all along their dorsal projections [25], our observations are consistent with the idea that LHLK neurons lie downstream of clock neurons.

Given the proximity of clock neurons and LHLKs, we wanted to test whether LK regulates circadian rhythms via LHLKs rather then the other LK-expressing neurons [19, 26]. We used *apterous-Gal4* to express Lk^{RNAi} in LHLKs but not in SELKs or Abdominal LK neurons (ABLKs) [26]. Since *apterous-Gal4* > Lk^{RNAi} flies had weaker rhythms than control flies (**Supplementary Table 2**), we propose that LK functions as a clock output specifically in

LHLK neurons. This function appears distinct from the roles of LK signaling in feeding and diuresis, which are likely mediated by the SELKs and ABLKs [18, 27].

The LK/LK-R circuit connects to locomotor and sleep areas

Since LHLK neurons contact LK-R neurons [18], we examined the projections of LK-R expressing neurons to determine which brain regions are the likely target of the LK/LK-R circuit. LK-R neurons form a dense and complex meshwork. However, a subset of LK-R neurons either project to or have cell bodies in brain regions implicated in controlling locomotion and/or sleep – specifically the PI and two regions of the Central Complex: the Ellipsoid Body (EB) and Fan-Shaped Body (FSB) [8, 9] (**Fig. 2f-g**). To visualize subsets of LK-R neurons, we generated flip-out FLEXAMP clones with *Lkr-Gal4*. We observed FLEXAMP GFP in the FSB in all 6 clones that labeled LK-R cell bodies in the lateral horn (**Fig. 2g**). These lateral horn LK-R neurons arborize in the posterior part of the brain and overlap extensively with LHLK projections (**Fig. 2h**). Moreover, these LK-R arborizations are likely inputs since they are enriched for DenMark staining (**Fig. 2i**) and these posterior regions of the brain are where the pre-synaptic marker Syt::GFP localizes in LHLKs (**Fig. 2d**). These data suggest that most LK-R neurons projecting to the FSB receive inputs from LHLKs. In contrast, LK-R outputs marked by Syt::GFP are primarily in the EB and FSB (**Fig. 2j-k**). LK-R outputs are also present in the SOG where SELKs are found (data not shown).

We found a second *Lkr-Gal4* line (*Lkr^{R65C07}-Gal4*) that also labels neurons in the lateral horn with pre-synaptic termini in the FSB (**Supplementary Fig. 3**). Using a *Lkr^{R65C07}-LexA* driver, we found that LK-R^{R65C07} projections in the FSB intermingle with projections from neurons labeled by 3 other FSB neuron Gal4 lines that affect locomotor activity and sleep [8, 28] (**Supplementary Fig. 3f**). Thus LHLKs and these lateral horn LK-R neurons have the appropriate anatomy to connect clock neurons with locomotor activity and sleep control centers.

LHLK neuron excitability is regulated by clock neurons

Next we used a functional approach to directly test connectivity and identify the direction of information transfer. We first manipulated s-LN$_v$ activity by expressing the mammalian ATP-gated cation channel P2X$_2$. Since *Drosophila* neurons do not express endogenous ATP-gated channels, ATP only activates neurons expressing the P2X$_2$ transgene [29]. We determined how this affects LHLK neuronal responses, using the genetically-encoded calcium indicator GCaMP6S [30] as a proxy for neuronal activity.

As a positive control, we first expressed P2X$_2$ and GCaMP6S in LN$_v$s and detected robust calcium transients in s-LN$_v$s after perfusing ATP onto explanted brains (**Supplementary Fig. 4a**). We saw similar responses in the large LN$_v$s (l-LN$_v$s) that regulate arousal [31, 32]. To measure responses in LHLKs, we used *Lk-Gal4* to express GCaMP6S and *Pdf-LexA* [32] to express P2X$_2$ in LN$_v$s. However, LN$_v$ activation did not detectably change GCaMP6S fluorescence in LHLK neurons (**Supplementary Fig. 4a**, red).

To test whether LN_vs inhibit LHLK neurons, we first needed to identify a way to activate LHLKs. We found that the acetylcholine agonist Carbachol (CCh) induces calcium transients in LHLKs in a dose-dependent manner (**Supplementary Fig. 4b**). We pre-incubated brains with Tetrodotoxin (TTX) to determine if this response is direct. TTX blocks most communication via neural circuits by preventing action potentials, although graded potentials are probably unaffected. The LHLK response to CCh persisted in the presence of TTX, suggesting that CCh directly activates LHLKs (**Supplementary Fig. 4b**).

We then tested whether the response of LHLKs to CCh is inhibited by LN_v activation, using a lower CCh concentration to be able to detect inhibition. We found that inducing LN_v firing almost completely abolished the LHLK response to CCh (**Fig. 3a**). This inhibition is specific since it requires $P2X_2$ expression in LN_vs (**Fig. 3a**). Thus LHLK neurons are functionally post-synaptic to the clock network, consistent with their anatomy (**Fig. 2**). Our results also reveal the sign of this connection: LHLKs are inhibited by LN_v activity.

CCh could generate calcium transients by activating muscarinic receptors to release internal calcium stores [33] or nicotinic receptors to depolarize the neurons and induce firing. To test whether LN_vs inhibit LHLKs via intracellular signaling or via membrane excitability, we added 35mM KCl to directly generate calcium transients in LHLKs by depolarization. We found that the response of LHLKs to KCl was strongly reduced when LN_vs were simultaneously activated (**Fig. 3b**). Thus clock neurons inhibit LHLKs at the level of membrane excitability.

Next, we asked whether PDF neuropeptide - the main LN_v output - is responsible for inhibiting LHLKs. PDF increases cAMP by activating the PDF Receptor (PDFR) in several classes of clock neurons including s-LN_vs and DN_{1p}s [16, 17]. We found that a 30 second PDF perfusion gradually increased intracellular calcium levels in s-LN_vs, consistent with PDF depolarizing s-LN_vs and DN_{1p}s [16, 17]. This response is specific since it was not observed in l-LN_vs (**Supplementary Fig. 4c)**, which do not express PDFR [34].

Although LHLK neurons were not detectably activated by PDF perfusion (**Supplementary Fig. 4c**), pre-incubating brains with PDF dramatically inhibited their CCh response (**Fig. 3c**). PDF inhibition was transient and disappeared after 15 min washout (**Supplementary Fig. 4d**). Thus PDF signaling can inhibit LHLKs, further evidence that LHLKs are downstream of the clock network.

However, since PDF can activate s-LN_vs and other clock neurons [16, 17, 34] (**Supplementary Fig. 4c**), our data do not determine if PDF directly controls LHLK excitability. To test this, we used two approaches. First, we used TTX to block action potentials while applying PDF. TTX was added for 20 min prior to PDF and also throughout the experiment. We found that TTX treatment largely eliminated LHLK inhibition by PDF (**Fig. 3c**), indicating that PDF acts indirectly on LHLKs. Second, we pre-incubated brains in PDF but this time with LN_vs ablated via a *Pdf-Dti* transgene [35]. This also prevented PDF from inhibiting LHLKs (**Fig. 3d**). Since PDF requires LN_vs to inhibit LHLKs, we interpret this to mean that PDF activates s-LN_vs (**Supplementary Fig. 4c**) which then signal to LHLKs either via an additional s-LN_v neurotransmitter [36] or indirectly via the clock network. Identifying the

neurons that directly regulate LHLKs will require finding the signal that modulates LHLK excitability.

LK peptide does not modulate LN_v excitability

We then determined how LK affects its target neurons. We first tested if LK-R neurons respond to LK peptide, focusing on the LK-R neurons with cell bodies in the lateral horn that project to the FSB. Adding LK to *Lkr > GCaMP6S* brains did not activate these LK-R neurons (**Supplementary Fig. 4e**). However, they were activated by CCh and this response was strongly reduced by pre-incubation in LK peptide (**Fig. 3e**). This contrasts with non-neuronal stellate cells where LK increases intracellular calcium [37] and could be explained by differential G protein coupling in distinct cell types. We conclude that the LK-R neurons in the lateral horn are *bona fide* LK-responding neurons. In addition, their projection patterns strongly suggest they are downstream of LHLKs but not SELKs. Therefore we propose that the LK/LK-R network connects clock neurons to the FSB and possibly also to the EB and PI.

We also tested whether LK feeds back on clock neurons. Since we found no evidence for LK activating LN_vs in *Pdf > GCaMP6S* brains (data not shown), we tested whether LN_vs can be inhibited by LK. LN_vs respond to CCh [38], but this response was unaffected by pre-incubating brains with LK (**Fig. 3f** and **Supplementary Fig. 4f**). Thus LK does not affect s-LN_v activity and LHLK neurons seem to act as outputs of the clock network.

Clock neurons impose rhythms on LHLK activity

LN_vs and DN_{1p}s are most depolarized and have highest spontaneous firing rates around dawn [39-41]. Since LHLK neuronal excitability is controlled by LN_V firing, we speculated that LHLK neuron activity is also rhythmic (**Fig. 3**). However, the timing of peak LN_v and LHLK activity should differ since LN_vs inhibit LHLKs..

To test these ideas, we first measured LHLK responses to CCh at two different times in DD. We measured LHLK responses during the subjective morning (CT0-3) when LN_v activity is high and the subjective evening (CT9-12) when LN_v activity is low [39] [CT: Circadian Time in DD after entrainment to a 12:12 Light:Dark cycle]. We maintained individual flies in the dark until dissection to minimize exposure to light. Strikingly, we found that the LHLK response to CCh was two-fold lower in the subjective morning than subjective evening and additional time points revealed a 24hr rhythm (**Fig. 4a-b**). Low LHLK excitability when LN_v activity is high is consistent with LN_vs inhibiting LHLK neurons. Oscillations in explanted brains indicate that these rhythms are not driven by locomotor activity.

LHLK excitability rhythms are likely clock-controlled since they persist in DD. To test this, we measured CCh responses in *period* null mutant flies (per^0) in which the molecular clock has stopped [1]. We found that changes in LHLK excitability were lost in per^0 mutants, showing that these rhythms require intact molecular clocks (**Fig. 4c-d**). This suggested that LHLK rhythms are imposed by circadian pacemaker neurons since LHLK neurons do not contain molecular clocks. We thus measured LHLK excitability rhythms in brains with LN_vs ablated and found this also eliminated LHLK rhythms (**Fig. 4e-f**).

To determine if these LHLK rhythms reflect endogenous neuronal activity, we quantified baseline GCaMP6S fluorescence in living explanted brains as a measure of spontaneous activity [42]. We observed a robust oscillation of GCaMP6S intensity with a peak around subjective dusk (CT11) and a trough at subjective dawn (CT0 and CT23, **Fig. 4g**). We did not see any changes in GFP intensity between CT0 and CT11 using a destabilized GFP transgene expressed with *Lk-Gal4* (**Fig. 4h,** as in ref. [43]). Thus the GCaMP6S oscillation is not due to rhythmic *Lk-Gal4* expression and presumably reflects changes in spontaneous LHLK activity over 24hr.

We also measured baseline GCaMP6S levels in LHLK neurons in per^0 mutants (**Fig. 4g**) and when LN_vs were ablated (**Fig. 4i**). Rhythms were lost in both situations, confirming that LHLK excitability is clock-controlled and driven by pacemaker neurons. We also found that artificially activating s-LN_vs in the evening by applying PDF peptide decreased baseline GCaMP6S levels in LHLKs (**Fig. 4j**). Thus we conclude that s-LN_v firing reduces LHLK neuronal activity. PDF did not reduce LHLK GCaMP6S to the trough levels observed at dawn. This could mean that either s-LN_v firing is required for >30min to fully inhibit LHLKs or that weaker s-LN_v synaptic outputs at dusk [43] prevent complete LHLK inhibition. In conclusion, these results demonstrate that LHLK excitability rhythms are generated non cell-autonomously by rhythmic signaling of the clock network.

LHLK activity rhythms propagate to LK-R neurons

Next we tested if LHLK activity rhythms are transmitted to LK-R neurons. We measured LK-R responses to CCh in DD and found that LK-R neurons are more excitable at dawn than dusk (**Fig. 5a-b**). Furthermore, LK-R excitability rhythms were abolished in per^0 mutants (**Fig. 5b-c**). We also measured LK-R excitability in Lkr^{c003} hypomorphs to test whether LK peptide itself transmits LHLK activity rhythms to LK-R neurons. We found that LK-R excitability oscillations were dampened in Lkr^{c003} mutant flies (**Fig. 5b,d**), consistent with the hypomorphic nature of this allele and with LK modulating LK-R neurons. Thus LK-R neuron excitability is rhythmic, clock-controlled and in antiphase to LHLKs, consistent with LK peptide inhibiting LK-R neuronal activity.

We also tested if these LK-R excitability rhythms reflect endogenous rhythms in neuronal activity by measuring baseline GCaMP6S levels. We observed a robust 24hr oscillation (**Fig. 5e**) in antiphase to LHLKs (compare **Fig. 4g**). This oscillation was clock-dependent (**Fig. 5e**) and blocked in *Pdf-Dti* brains (**Fig. 5f**), demonstrating that it originates from pacemaker neurons.

We also used Lkr^{R65C07}-*Gal4* line to drive *GCaMP6S* in the LK-R neuronal subset that projects to the FSB (see **Supplementary Fig. 3**). These neurons also respond to LK peptide (**Supplementary Fig. 4g**) and their baseline GCaMP6S levels oscillate in phase with *Lkr-Gal4* (**Supplementary Fig. 4h**), confirming that both *Lkr-Gal4* lines label the same neurons. Thus rhythmic pacemaker neuron activity is propagated at least two layers deeper into the brain to generate non cell-autonomous rhythms in LK-R neurons via LK signaling.

LK and LK-R neurons control locomotor activity and sleep

Rhythms in LHLK and LK-R activity suggest that the clock network imposes rhythmic neuronal activity on locomotor and sleep control centers. To test if these neuronal rhythms are important for behavioral rhythms, we manipulated LK and LK-R neuronal activity. To manipulate the subset of LK-R neurons most likely to receive LHLK inputs, we used the more restricted *Lkr^{R65C07}-Gal4*. We activated LK and LK-R^{R65C07} neurons for 4 days using a UAS transgene expressing the heat-activated cation channel dTrpA1, which is inactive below 25°C [44]. After entraining to LD cycles at 19°C, flies were assayed in DD for 4 days at 19°C and then for 4 days at 28°C. Control flies had stronger rhythms at 28°C than 19°C, as seen previously [10, 43]. In contrast, activating LK neurons weakened behavioral rhythms at 28°C compared to 19°C, while activating LK-R^{R65C07} neurons blocked the increase in rhythm strength at 28°C (**Fig. 6a** and **Supplementary Table 2**). These data suggest that LK/LK-R neuronal activity rhythms are required for normal behavioral rhythms.

To explore the effect of LK and LK-R neurons in more detail, we performed 1-day activation experiments and also used the temperature-sensitive dominant negative Dynamin (*UAS-shi^{ts}*) to block synaptic outputs [45]. Control flies increased their activity levels in response to heat (grey and black lines in **Fig. 6b**). This was due to increased locomotor activity while awake and decreased sleep (**Supplementary Fig. 5a-d**). In contrast, activating LK neurons dramatically reduced locomotor activity levels (**Fig. 6b**) by increasing the amount of sleep and reducing activity levels while awake (**Supplementary Fig. 5a,c**). Since *Lk > dTrpA1* flies recovered similar activity and sleep levels to control flies on returning to 19°C, activating LK neurons does not permanently alter locomotor and sleep circuit function or render flies unhealthy (**Fig. 6b** and **Supplementary Fig. 5a,c**).

Activating LK-R^{R65C07} neurons had the opposite effect to activating LK neurons, with increased locomotor activity and decreased sleep compared to controls (**Fig. 6b** and **Supplementary Fig. 5b**). This effect was shorter-lived than for LK neurons and was most apparent during the first 6hr of the temperature shift (lower panel in **Fig. 6b**, quantified in **Supplementary Fig. 5d**). The opposite effects of activating LK and LK-R neurons are consistent with LK inhibiting LK-R excitability (**Fig. 3**) and indicate that LK neurons control locomotor activity and sleep levels by inhibiting LK-R neurons.

We then inhibited synaptic transmission from LK and LK-R^{R65C07} neurons with *shi^{ts}*. Surprisingly, inhibiting LK neuron synaptic transmission had almost no effect on locomotor activity or sleep (**Fig. 6c** and **Supplementary Fig. 5e**). One possible explanation is that LK neurons control these behaviors via neuropeptide signaling, which may be Dynamin-independent [46]. Indeed, constitutively hyper-polarizing LK neurons with the inward rectifier potassium channel *Kir2.1* [47] significantly reduced locomotor rhythm strength (**Supplementary Table 2**).

In contrast, inhibiting synaptic transmission from LK-R^{R65C07} neurons reduced locomotor activity and increased sleep (**Fig. 6c** and **Supplementary Fig. 5f**). This effect is the opposite of LK-R^{R65C07} activation and similar to activating LK neurons (**Fig. 6b**). These data further support the model that LK neurons inhibit LK-R neurons which normally promote

locomotor activity and inhibit sleep. These results also show that LK-R neuron signaling is required by day for normal levels of locomotor activity and sleep.

We repeated the experiments with LK-R^{R65C07} neurons with a heat pulse starting at CT12 and obtained very similar results to CT0-24 heat pulses: LK-R^{R65C07} neuron activation and inhibition mainly affected behavior during subjective day (data not shown). Thus LK-R neurons seem competent to control locomotor and sleep only at times when they are most excitable (see **Fig. 5)**. The absence of phenotypes at night could be due to masking effects by heat and/or interactions with other neural pathways that override the effects of LK-R signaling during subjective night. Indeed, light dramatically delayed the effects of LK and LK-R^{R65C07} neuron activation and inhibition on locomotor activity during the day (**Supplementary Fig. 6a**). This suggests that one or more pathways downstream of light at least partially suppress the effects of interfering with LK-R neuron signaling. Thus LK-R neuron outputs are likely integrated with other pathways to shape behavioral rhythms.

LK-R expressed in Malphigian tubule stellate cells responds to circulating LK peptide released from ABLKs to regulate diuresis [37]. To test if the *dTrpA1* locomotor activity phenotypes are require neuronal expression, we added *elav-Gal80* to eliminate *dTrpA1* expression from neurons in *Lk > dTrpA1* and *Lkr^{R65C07} > dTrpA1* flies. Restricting *dTrpA1* expression to non-neuronal tissues completely abolished locomotor activity and sleep phenotypes (**Supplementary Fig. 6b**). Thus the LK and LK-R cells controlling locomotion and sleep are neurons. Together with LK/LK-R anatomy and our functional imaging experiments, these behavioral data implicate the brain LK/LK-R circuit as a critical circadian output that regulates rhythmic locomotor activity and sleep.

Rhythms propagate in a second clock output circuit

Finally we examined a second group of clock output neurons – the DH44-expressing neurons in the PI that do not express molecular clock components but receive inputs from DN_{1p} clock neurons [10]. We found that baseline GCaMP6S levels oscillate in DH44 neurons and this requires LN_vs (**Fig. 7**). Thus rhythmic DH44 neuron activity is also imposed by pacemaker neurons. We propose that non-autonomous propagation of neuronal rhythms is a general mechanism for transmitting pacemaker neuron information.

DISCUSSION

How does the clock network regulate downstream circuits? We show that the LHLK, LK-R and DH44 neurons downstream of the *Drosophila* clock network display clock-dependent activity rhythms in explanted brains although these neurons have no molecular clocks themselves. The loss of LHLK, LK-R and DH44 neuronal activity rhythms after LN_v ablation demonstrates that these rhythms originate from pacemaker neurons (see **Supplementary Fig. 7**). In addition, PDFR-expressing neurons in the EB display a circadian rhythm in their cAMP response to acetylcholine which partly depends on PDF [14]. Thus clock output pathways relay rhythmic information to several different brain regions using diverse signals.

Function of LK/LK-R signaling

Behavioral analyses of *Lk* and *Lkr* mutants and neuronal manipulations implicate the LK/LK-R circuit in organizing locomotor activity and sleep over time. Specifically, we found that LK-R neurons promote locomotor activity and reduce sleep (**Fig. 6**). This function seems distinct from the diuretic function of LK/LK-R signaling which is likely controlled by LK release from ABLKs [19]. Indeed, we found that locomotor behavior was disrupted with RNAi targeting LK only in LHLKs but not in SELKs and ABLKs and also when manipulating LK-R specifically in neurons. Other functions of LK/LK-R signaling such as regulating feeding [18] are unlikely to affect locomotor rhythms since *Lk* and *Lkr* mutants ingest normal amounts of food [18] and since blocking feeding rhythms does not alter locomotor activity rhythms [7]. However, we cannot completely rule out that LK/LK-R regulation of feeding affects locomotor and sleep behaviors given the precedent of orexin/hypocretins regulating both energy intake and arousal in vertebrates [48].

LK-R neurons intermingle with neurons that promote locomotor activity in the FSB [8, 28]. However, LK-R neurons projecting to other locomotor centers such as the PI and EB might also contribute to circadian behavior. The locomotor activity-promoting role of LK-R neurons is consistent with their neuronal activity profile determined by GCaMP: they are more excitable and active around dawn, when flies have high locomotor activity. Together with our analysis of LHLK and pacemaker neuron connections, these observations suggest a model in which signaling from the clock network inhibits LHLK neurons at dawn to allow LK-R neurons to signal and promote locomotor activity (**Supplementary Fig. 7**). Supporting this model, downregulating *Lk* and *Lkr* by RNAi interferes with morning anticipatory behavior but has no effect in the evening (data not shown).

In addition to being inhibited by LHLKs at dusk/night, we found evidence suggesting that LK-R neuron outputs are blocked by additional unidentified signaling pathways since activating them at night did not affect locomotor behavior. Some of these pathways may be downstream of light, which partially suppresses LK-R-driven locomotor activity during the day. The exact timing of LK and LK-R firing likely also depends on additional non-circadian inputs and probably differs from the windows of excitability imposed by clock neurons. Additional work will be required to determine how the different circuits downstream of the clock interact to organize circadian behaviors.

In conclusion, our experiments reveal a mechanism to temporally control behavior: Pacemaker neuron electrical rhythms are propagated through downstream neuronal circuits that control specific components of circadian behavior.

ONLINE METHODS

Fly strains

The following *Drosophila melanogaster* fly strains have been described previously: y^1 w^{1118}; ; Lk^{c275} (ref. [18]), y^1 w^{1118}; ; Lkr^{c003} (ref. [18]), *y w; ;* Lkr^{Mimic1} (MI06336), *y w; ;* Lkr^{Mimic2} (MI08640), w^{1118} ; ; *Df(3L)BSC371* (ref. [49]), w^{1118}; ; *Df(3L)BSC372* (ref. [49]), w^{1118}; ; *Df(3L)BSC557* (ref. [49]), *y w; Lk-Gal4* (ref. [19]), *y w; ; Lkr-Gal4* (ref. [18]), $Pdf_{0.5}$-*Gal4* (ref. [50]), *tim(UAS)-Gal4* (referred to here as *tim-Gal4* , ref. [51]), *per-Gal4* (ref. [52]), *Ap-*

Gal4^{MD544} (ref. [53]), *UAS-nlsGFP* (from C. Desplan), *elav-Gal4; UAS-Dcr-2* (ref. [54, 55], the *UAS-Dcr-2* transgene was included to enhance RNAi effectiveness), *y*^{1} *v*^{1}*; ; UAS-Lk*^{RNAi} (TRiP JF01816), *y*^{1} *v*^{1}*; ; UAS-Lkr*^{RNAi} (TRiP JF01956), *10×UAS-mCD8::GFP* (ref. [56]), *FLEXAMP* cassette: y w, UAS-Flp; tub-Gal80^{ts} / CyO ; act-FRT-stop, y^{+}-FRT-LexA, 13×lexAop-myr-GFP (ref. [21]), *Clk4.1-Gal4* (ref. [57]), *Mai179-Gal4 ; PdfGal80* (ref. [58, 59]), *w; L / CyO; UAS-Syt::GFP, UAS-DenMark* (ref. [23]), *w; UAS-cycΔ* (ref. [20]), *w; 20×UAS-GCaMP6S* (ref. [30]), *w; ; Pdf-LexA, lexAop-P2X*$_2$ (ref. [60]), *y per*^{0} *w*; (ref. [61]), *Pdf-Dti* (ref. [35], we verified that *Pdf-Dti* ablates all adult LN$_v$s by immunostaining, n=8 brains, data not shown), *UAS-dsGFP* (ref. [62]), *DH44-VT-Gal4* VDRC (ref. [10]), *w*^{1118}*;; UAS-Kir2.1* (ref. [47]), *w; UAS-dTrpA1* (ref. [44]), *+;UAS-shi*^{ts}*; UAS-shi*^{ts} (ref. [45]), *w*^{1118}*; ; Lkr*^{R65C07}*-Gal4* and *w*^{1118}*; ; Lkr*^{R65C07}*-LexA* (ref. [63], Janelia R65C07), *121Y-Gal4*, *C5-Gal4*, *c584-Gal4*, described in ref. [8, 28], *elav-Gal80* (from S. Sweeney, ref. [64]).

Behavioral analyses

Flies were raised on regular cornmeal medium and entrained to 12:12hr LD cycles for at least 3 days before transfer to DD. Flies were raised and assayed at 25°C except for experiments involving *UAS-dTrpA1* or *UAS-shi*^{ts} in which flies were raised at 19°C and assayed at 19°C and 28°C. Male flies assayed for behavior were ~5-10 days old. No randomization or blinding was used when preparing and analyzing behavioral experiments, but controls were performed in parallel. Locomotor activity was recorded using the DAM system (TriKinetics, Waltham, MA). Manual inspection of actograms was performed for each fly to exclude flies that died during an experiment. Rhythm strength (power) and period were analyzed by ClockLab in Matlab using chi-squared analysis. All other analyses (actograms, activity and sleep profiles, total activity and waking activity) and statistical tests were performed using custom-written scripts in IgorPro (Wavemetrics) as in ref. [65]. Sleep was defined as at least 5 min of inactivity: 0 beam crossings in a 5 min data window.

Minimum required sample sizes were determined empirically, no statistical methods were used. Behavioral experiments were repeated at least twice. The RNAi screen was initially performed with 8 flies but genotypes with potentially interesting phenotypes repeated to obtain >16 flies. For *dTrpA1* and *shi*^{ts} experiments, larger sample sizes were required since most experimental treatments lasted only one day. Thus these experiments were performed with 32 flies at least twice. To determine which statistical test to compare experimental flies to parental controls, we first ran Levene's test to determine if variances were equal and found that they were often unequal. Thus we used the non-parametric Kolmogorov-Smirnov test (KS test) to determine if experimental flies differed from controls. *dTrpA1* or *shi*^{ts} manipulations were considered to have a significant effect when experimental flies were statistically different from both controls ($p<0.05$).

Immunocytochemistry

Adult brains were dissected in PBS, fixed for 45 min in 4% formaldehyde in PBS, rinsed 3x in PBS + 1% Triton and washed for ~2hr in PBS + 1% Triton. Primary antibodies were incubated in PBS + 0.5% Triton + 4% horse serum overnight at 4°C. Secondary antibodies were incubated for 2hr at room temperature and rinsed overnight at 4°C. Brains were mounted in SlowFade (Invitrogen). Primary antibodies used were: rabbit anti-LK at either

1:1000 or 1:10000 for quantification (ref. [18]), mouse anti-PDF 1:50 (ref. [66]), rat anti-TIM 1:250 (from A. Sehgal), Guinea Pig anti-VRI 1:1500 (from P. Hardin), sheep anti-GFP 1:500 (Novus Biologicals NB100-62622), rabbit anti-RFP 1:500 (Invitrogen R10367) and mouse anti-RFP 1:100 (MBL 8D6). Alexa Fluor (Invitrogen) secondary antibodies were all used at 1:200. Confocal stacks were acquired with a Leica SP5 confocal microscope with a 20x water immersion objective and processed in ImageJ. Anatomical analyses were performed on male and female flies (~2-10 days old), with a minimum of 8 brains imaged on both left and right sides for each experiment. Anatomical observations were highly reproducible from brain to brain.

TIM staining in **Fig. 1** were performed in brains dissected at ZT22 (TIM levels high in clock neurons) except for DN_2s where brains were dissected at ZT10 (**Fig. 1i)**. Flip-out FLEXAMP clones (**Fig. 2g**) were generated with *tub-Gal80^{ts}*; *Lkr-Gal4* by transferring developing larvae at 29°C for ~3hr to allow transient *UAS-Flp* expression from *Lkr-Gal4*.

Protein level quantification was performed on ~3-5 day old male flies entrained to LD cycles. Quantification of LK, VRI and TIM levels in wild type and *Lk* mutants and of dsGFP in wild type flies were performed using IgorPro (Wavemetrics) on 8-bit images (i.e. pixel intensity ranging from 0-255). Average pixel intensity (integrated intensity / area) was measured for individual cell bodies using manually-defined ROIs on z projections. Background intensity was measured for each image and subtracted from the corresponding cell bodies. Sample sizes were determined empirically based on the relatively low variability observed between brains as previously [65]. We imaged 8 brains (16 LHLK cell bodies) to quantify LK levels in **Supplementary Fig. 1b,c** and 9-10 brains (>60 cell bodies) for TIM and VRI in **Supplementary Fig. 2c-e** for each data point. To quantify LK levels in *Lk^{RNAi}* brains, LHLK cell bodies were first identified using higher laser power since they were almost undetectable and then imaged using regular acquisition settings. s-LN_vs were identified using PDF staining and distinguished from l-LN_vs by size. No randomization or blinding was used when preparing and analyzing immunostaining.

Quantitative Real Time PCR (qPCR)

Lkr mRNA levels were measured by qPCR using a standard curve constructed as in ref. [67]. RNA was extracted from male whole heads (40 heads/extraction, flies 3-5 days old) using PureLink RNA Mini Kit (Ambion). Sample sizes were based on ref. [67]. Each data point consisted of 2 biological replicates with 3 technical replicates (6 samples total). No randomization or blinding was used when preparing and analyzing qPCR. Reactions were performed using the LightCycler RNA Master HybProbe kit (Roche) with Calmodulin as a loading control [43]. Primers and probes were synthesized by TIB Molbiol (Adelphia, NJ).

Lkr-F: AAATGCGGACCGTGACA

Lkr-R: GGACGTGCCCTAAGTGGAT

Lkr-FL: GGTATTCACGCTGACCGCCA--FL

Lkr-LC: LC640-TGCAATCGATCGGCATAGGGCC--PH

Calcium imaging

We chose the GCaMP6S variant for two reasons. First, GCaMP6S has slower kinetics than GCaMP6F and GCaMP6M [30], which makes it easier to detect calcium transients in many neurons in a large field of view at slow scanning speed – even though the slow time course of GCaMP6S responses (>5min) is not physiological. Second, GCaMP6S is more sensitive than GCaMP6F and GCaMP6M [30], making it easier to detect subtle changes in neuronal activity, especially for baseline GCaMP6S fluorescence.

3-5 day old adult male flies entrained to LD cycles were anesthetized on ice and dissected in hemolymph-like saline (HL3, ref. [34]). For measuring GCaMP6S responses to drugs, brains were gently pressed against a glass slide coated with Poly-L Lysine (Sigma) and mounted in a Bioptechs FCS3 perfusion chamber. HL3 flow across the brain was established and maintained at ~1ml/min by gravity. Brains were allowed to recover for ~5min in the chamber before an experiment. Test compounds (0.5ml) were injected into the tubing system using a syringe and 3-way stopcock. Compounds were perfused for ~30sec and started at slightly different times depending on experiments because of small changes in flow rate and tubing length. The timing of drug perfusion is indicated by the position of the grey bar on GCaMP6S line graphs. To measure baseline GCaMP6S intensity, live brains were mounted in HL3 medium on glass slides coated with Poly-L Lysine and imaged immediately in one z-stack. No randomization or blinding was used when preparing and analyzing calcium imaging experiments.

ATP (Sigma) and Carbachol (Sigma) were dissolved directly in HL3. KCl was used at 35mM after ref. [68]. PDF and LK peptides were synthesized by PolyPeptide Group (San Diego, CA), dissolved in DMSO, diluted to final concentration in HL3 and used within 1 day. Three different batches of PDF were used during this study and had different efficacies, as previously noted [14]. The batch used in **Supplementary Fig. 4d** was more potent and thus used at lower concentration (20 μM) than the batches used in **Fig. 3c-d** (100 μM).

TTX (Tetrodotoxin citrate, Abcam) was dissolved in HL3 and included in the main HL3 flow throughout the relevant experiments and while test compounds were injected. Electrophysiological recordings of l-LN_v neurons show that TTX completely eliminates action potentials within 1 min of application on brain explants [40]. We used a high TTX concentration to completely inhibit action potentials as in ref. [38, 69]. TTX works in our preparation since it eliminates the inhibitory effect of PDF on LHLKs (see **Fig. 3c**).

Pre-incubation with PDF, LK or TTX was in a 1ml drop/well of HL3 prior to mounting in the chamber. For the PDF+TTX experiment (**Fig. 3c**), brains were first incubated for 20 min in TTX and then for another 20 min in PDF+TTX (or vehicle+TTX). PDF washout (**Supplementary Fig. 4d**) was performed in the perfusion chamber after the first CCh stimulation.

GCaMP6S imaging was performed with an Olympus two-photon system with a Mai-Tai laser (Spectra Physics) at 920 nm and a 10x water immersion objective. z stacks (~20 slices at 5 μm intervals) were acquired every 30 seconds for 10 minutes. Maximal z projections were used to quantify fluorescence in individual neuronal cell bodies over time. 12-bit

images were used (i.e. pixel intensity ranging from 0-4095). Subsequent data processing was performed using custom-written scripts in IgorPro (Wavemetrics). Individual traces were normalized to initial fluorescence (F/F_0) and averaged across samples. The line graphs show the average GCaMP6S fluorescence (thick line) +/− standard error of the mean (thin vertical lines) plotted versus time. The mean maximum change in GCaMP6S fluorescence (Max. $\Delta F/F_0$) was calculated by averaging the peak F/F_0 determined for each trace of a given sample. For each experiment, the sample sizes are indicated as n=x;y where x and y are the total number of cell bodies and brains quantified per sample, respectively. No statistical method was used to determine minimum required sample sizes, they were based on ref. [38] and also determined empirically. Generally, 8 brains were imaged for each data point over at least two experiments performed on different days. Additional brains were imaged when the results were variable from one day to another and all results pooled for analysis. We verified that the difference in Max. $\Delta F/F_0$ between samples was due to differences in absolute peak GCaMP6S intensity, not to differences in initial GCaMP6S intensity for each experiment.

Statistics were performed in IgorPro (Wavemetrics). Since samples often had unequal variances, we used the KS test to compare responses to drugs to avoid the problem of requiring normal distributions and equal variances. For baseline GCaMP6S experiments, we used Kruskal-Wallis ANOVA to determine if there was a significant rhythm in the data.

Low expression levels from *Lk-Gal4* meant that we used flies homozygous for both *Lk-Gal4* and *UAS-GCaMP6S* to image GCaMP6S in LHLKs, except for *Pdf-Dti* experiments. For the latter, we decreased the scan speed (1 z-stack per minute) to compensate for decreased signal intensity. To measure LHLK, LK-R and DH44 neuron excitability rhythms and baseline GCaMP6S levels in DD, flies were entrained to LD for at least 3 days and assayed on the first day in DD. Individual flies were maintained in DD and anesthetized on ice immediately before dissection under visible light. In total, brains were exposed to visible light for <5 min before measuring excitability and for between 5-10min before measuring baseline GCaMP6S.

Supplementary Material

Refer to Web version on PubMed Central for supplementary material.

ACKNOWLEDGEMENTS

We thank B. Al-Anzi (Caltech), D. Clark (Yale University), P. Hardin (Texas A & M), P. Herrero (Universidad Autónoma de Madrid), M. Rosbash (Brandeis University), F. Rouyer (Institut des Neurosciences Paris-Saclay), A. Sehgal (U Penn School of Medicine), O. Shafer (University of Michigan), S. Sweeney (University of York), the DSHB and the Bloomington stock center for flies and antibodies. We thank the TRiP stock center at Harvard Medical School (NIH/NIGMS R01-GM084947) for transgenic RNAi fly stocks. We thank C. Desplan for sharing the two-photon microscope and perfusion chamber and O. Shafer for advice on calcium imaging. We thank R. Behnia, C. Desplan, C. Hackley, E. Meekhof, A. Petsakou, H. Piggins and Z. Zhu for discussions and comments on the manuscript. We also thank our anonymous reviewers for suggesting that we measure baseline GCaMP6S levels. This investigation was conducted in facilities constructed with support from Research Facilities Improvement Grant Number C06 RR-15518-01 from the National Center for Research Resources, National Institutes of Health. Imaging was performed at the NYU Center for Genomics & Systems Biology. This work was supported by EMBO ALTF 249-2009 (MC), the Charles H. Revson foundation (MC), EMBO ALTF 680-2009 (CB), HSFPO LT000077/2010-L (CB), NIH grant R01 EY017916 (to C. Desplan), NIH grant GM063911 (JB) and the NYU Abu Dhabi Research Institute (G1205).

REFERENCES

1. Herzog ED. Neurons and networks in daily rhythms. Nat Rev Neurosci. 2007; 8:790–802. [PubMed: 17882255]
2. Nitabach MN, Taghert PH. Organization of the *Drosophila* circadian control circuit. Curr Biol. 2008; 18:R84–93. [PubMed: 18211849]
3. Colwell CS. Linking neural activity and molecular oscillations in the SCN. Nat Rev Neurosci. 2011; 12:553–569. [PubMed: 21886186]
4. Dibner C, Schibler U, Albrecht U. The mammalian circadian timing system: organization and coordination of central and peripheral clocks. Annu Rev Physiol. 2010; 72:517–549. [PubMed: 20148687]
5. Morin LP. Neuroanatomy of the extended circadian rhythm system. Exp Neurol. 2013; 243:4–20. [PubMed: 22766204]
6. Myers EM, Yu J, Sehgal A. Circadian control of eclosion: interaction between a central and peripheral clock in *Drosophila melanogaster*. Curr Biol. 2003; 13:526–533. [PubMed: 12646138]
7. Xu K, Zheng X, Sehgal A. Regulation of feeding and metabolism by neuronal and peripheral clocks in *Drosophila*. Cell Metab. 2008; 8:289–300. [PubMed: 18840359]
8. Martin JR, Raabe T, Heisenberg M. Central complex substructures are required for the maintenance of locomotor activity in *Drosophila melanogaster*. J Comp Physiol A. 1999; 185:277–288. [PubMed: 10573866]
9. Foltenyi K, Greenspan RJ, Newport JW. Activation of EGFR and ERK by rhomboid signaling regulates the consolidation and maintenance of sleep in *Drosophila*. Nat Neurosci. 2007; 10:1160–1167. [PubMed: 17694052]
10. Cavanaugh DJ, Geratowski JD, Wooltorton JR, Spaethling JM, Hector CE, Zheng X, Johnson EC, Eberwine JH, Sehgal A. Identification of a circadian output circuit for rest:activity rhythms in *Drosophila*. Cell. 2014; 157:689–701. [PubMed: 24766812]
11. Martin JR, Ernst R, Heisenberg M. Mushroom bodies suppress locomotor activity in *Drosophila melanogaster*. Learn Mem. 1998; 5:179–191. [PubMed: 10454382]
12. Pitman JL, McGill JJ, Keegan KP, Allada R. A dynamic role for the mushroom bodies in promoting sleep in *Drosophila*. Nature. 2006; 441:753–756. [PubMed: 16760979]
13. Joiner WJ, Crocker A, White BH, Sehgal A. Sleep in *Drosophila* is regulated by adult mushroom bodies. Nature. 2006; 441:757–760. [PubMed: 16760980]
14. Pirez N, Christmann BL, Griffith LC. Daily rhythms in locomotor circuits in *Drosophila* involve PDF. J Neurophysiol. 2013; 110:700–708. [PubMed: 23678016]
15. Kunst M, Hughes ME, Raccuglia D, Felix M, Li M, Barnett G, Duah J, Nitabach MN. Calcitonin gene-related peptide neurons mediate sleep-specific circadian output in *Drosophila*. Curr Biol. 2014; 24:2652–2664. [PubMed: 25455031]
16. Seluzicki A, Flourakis M, Kula-Eversole E, Zhang L, Kilman V, Allada R. Dual PDF signaling pathways reset clocks via TIMELESS and acutely excite target neurons to control circadian behavior. PLoS Biol. 2014; 12:e1001810. [PubMed: 24643294]
17. Choi C, Cao G, Tanenhaus AK, McCarthy EV, Jung M, Schleyer W, Shang Y, Rosbash M, Yin JC, Nitabach MN. Autoreceptor control of peptide/neurotransmitter corelease from PDF neurons determines allocation of circadian activity in *Drosophila*. Cell Rep. 2012; 2:332–344. [PubMed: 22938867]
18. Al-Anzi B, Armand E, Nagamei P, Olszewski M, Sapin V, Waters C, Zinn K, Wyman RJ, Benzer S. The Leucokinin pathway and its neurons regulate meal size in *Drosophila*. Curr Biol. 2010; 20:969–978. [PubMed: 20493701]
19. de Haro M, Al-Ramahi I, Benito-Sipos J, Lopez-Arias B, Dorado B, Veenstra JA, Herrero P. Detailed analysis of Leucokinin-expressing neurons and their candidate functions in the *Drosophila* nervous system. Cell Tissue Res. 2010; 339:321–336. [PubMed: 19941006]
20. Tanoue S, Krishnan P, Krishnan B, Dryer SE, Hardin PE. Circadian clocks in antennal neurons are necessary and sufficient for olfaction rhythms in Drosophila. Curr Biol. 2004; 14:638–649. [PubMed: 15084278]

21. Bertet C, Li X, Erclik T, Cavey M, Wells B, Desplan C. Temporal patterning of neuroblasts controls Notch-mediated cell survival through regulation of Hid or Reaper. Cell. 2014; 158:1173–1186. [PubMed: 25171415]
22. Helfrich-Forster C. Neurobiology of the fruit fly's circadian clock. Genes Brain Behav. 2005; 4:65–76. [PubMed: 15720403]
23. Nicolai LJ, Ramaekers A, Raemaekers T, Drozdzecki A, Mauss AS, Yan J, Landgraf M, Annaert W, Hassan BA. Genetically encoded dendritic marker sheds light on neuronal connectivity in *Drosophila*. Proc Natl Acad Sci U S A. 2010; 107:20553–20558. [PubMed: 21059961]
24. Zhang YQ, Rodesch CK, Broadie K. Living synaptic vesicle marker: synaptotagmin-GFP. Genesis. 2002; 34:142–145. [PubMed: 12324970]
25. Gorostiza EA, Depetris-Chauvin A, Frenkel L, Pirez N, Ceriani MF. Circadian pacemaker neurons change synaptic contacts across the day. Curr Biol. 2014; 24:2161–2167. [PubMed: 25155512]
26. Herrero P, Magarinos M, Torroja L, Canal I. Neurosecretory identity conferred by the *apterous* gene: lateral horn Leucokinin neurons in *Drosophila*. J Comp Neurol. 2003; 457:123–132. [PubMed: 12541314]
27. Cognigni P, Bailey AP, Miguel-Aliaga I. Enteric neurons and systemic signals couple nutritional and reproductive status with intestinal homeostasis. Cell Metab. 2011; 13:92–104. [PubMed: 21195352]
28. Kahsai L, Martin JR, Winther AM. Neuropeptides in the *Drosophila* central complex in modulation of locomotor behavior. J Exp Biol. 2010; 213:2256–2265. [PubMed: 20543124]
29. Lima SQ, Miesenbock G. Remote control of behavior through genetically targeted photostimulation of neurons. Cell. 2005; 121:141–152. [PubMed: 15820685]
30. Chen TW, Wardill TJ, Sun Y, Pulver SR, Renninger SL, Baohan A, Schreiter ER, Kerr RA, Orger MB, Jayaraman V, Looger LL, Svoboda K, Kim DS. Ultrasensitive fluorescent proteins for imaging neuronal activity. Nature. 2013; 499:295–300. [PubMed: 23868258]
31. Sheeba V, Fogle KJ, Kaneko M, Rashid S, Chou YT, Sharma VK, Holmes TC. Large ventral lateral neurons modulate arousal and sleep in *Drosophila*. Curr Biol. 2008; 18:1537–1545. [PubMed: 18771923]
32. Shang Y, Griffith LC, Rosbash M. Light-arousal and circadian photoreception circuits intersect at the large PDF cells of the *Drosophila* brain. Proc Natl Acad Sci U S A. 2008; 105:19587–19594. [PubMed: 19060186]
33. Yagodin S, Pivovarova NB, Andrews SB, Sattelle DB. Functional characterization of thapsigargin and agonist-insensitive acidic Ca^{2+} stores in *Drosophila melanogaster* S2 cell lines. Cell Calcium. 1999; 25:429–438. [PubMed: 10579054]
34. Shafer OT, Kim DJ, Dunbar-Yaffe R, Nikolaev VO, Lohse MJ, Taghert PH. Widespread receptivity to neuropeptide PDF throughout the neuronal circadian clock network of *Drosophila* revealed by real-time cyclic AMP imaging. Neuron. 2008; 58:223–237. [PubMed: 18439407]
35. Gong Z, Liu J, Guo C, Zhou Y, Teng Y, Liu L. Two pairs of neurons in the central brain control *Drosophila* innate light preference. Science. 2010; 330:499–502. [PubMed: 20966250]
36. Frenkel L, Ceriani MF. Circadian plasticity: from structure to behavior. Int Rev Neurobiol. 2011; 99:107–138. [PubMed: 21906538]
37. O'Donnell MJ, Rheault MR, Davies SA, Rosay P, Harvey BJ, Maddrell SH, Kaiser K, Dow JA. Hormonally controlled chloride movement across *Drosophila* tubules is via ion channels in stellate cells. Am J Physiol. 1998; 274:R1039–1049. [PubMed: 9575967]
38. Lelito KR, Shafer OT. Reciprocal cholinergic and GABAergic modulation of the small ventrolateral pacemaker neurons of *Drosophila*'s circadian clock neuron network. J Neurophysiol. 2012; 107:2096–2108. [PubMed: 22279191]
39. Cao G, Nitabach MN. Circadian control of membrane excitability in *Drosophila melanogaster* lateral ventral clock neurons. J Neurosci. 2008; 28:6493–6501. [PubMed: 18562620]
40. Sheeba V, Gu H, Sharma VK, O'Dowd DK, Holmes TC. Circadian- and light-dependent regulation of resting membrane potential and spontaneous action potential firing of *Drosophila* circadian pacemaker neurons. J Neurophysiol. 2008; 99:976–988. [PubMed: 18077664]

41. Flourakis M, Kula-Eversole E, Hutchison AL, Han TH, Aranda K, Moose DL, White KP, Dinner AR, Lear BC, Ren D, Diekman CO, Raman IM, Allada R. A conserved bicycle model for circadian clock control of membrane excitability. Cell. 2015; 162:836–848. [PubMed: 26276633]
42. Bushey D, Tononi G, Cirelli C. Sleep- and wake-dependent changes in neuronal activity and reactivity demonstrated in fly neurons using in vivo calcium imaging. Proc Natl Acad Sci U S A. 2015; 112:4785–4790. [PubMed: 25825756]
43. Petsakou A, Sapsis TP, Blau J. Circadian rhythms in Rho1 activity regulate neuronal plasticity and network hierarchy. Cell. 2015; 162:823–835. [PubMed: 26234154]
44. Pulver SR, Pashkovski SL, Hornstein NJ, Garrity PA, Griffith LC. Temporal dynamics of neuronal activation by Channelrhodopsin-2 and TRPA1 determine behavioral output in *Drosophila* larvae. J Neurophysiol. 2009; 101:3075–3088. [PubMed: 19339465]
45. Kitamoto T. Conditional modification of behavior in *Drosophila* by targeted expression of a temperature-sensitive shibire allele in defined neurons. J Neurobiol. 2001; 47:81–92. [PubMed: 11291099]
46. Merighi A. Costorage and coexistence of neuropeptides in the mammalian CNS. Prog Neurobiol. 2002; 66:161–190. [PubMed: 11943450]
47. Baines RA, Uhler JP, Thompson A, Sweeney ST, Bate M. Altered electrical properties in *Drosophila* neurons developing without synaptic transmission. J Neurosci. 2001; 21:1523–1531. [PubMed: 11222642]
48. Gao XB, Horvath T. Function and dysfunction of hypocretin/orexin: an energetics point of view. Annu Rev Neurosci. 2014; 37:101–116. [PubMed: 24821311]

Methods-only references

49. Cook RK, Christensen SJ, Deal JA, Coburn RA, Deal ME, Gresens JM, Kaufman TC, Cook KR. The generation of chromosomal deletions to provide extensive coverage and subdivision of the *Drosophila melanogaster* genome. Genome Biol. 2012; 13:R21. [PubMed: 22445104]
50. Park JH, Helfrich-Forster C, Lee G, Liu L, Rosbash M, Hall JC. Differential regulation of circadian pacemaker output by separate clock genes in *Drosophila*. Proc Natl Acad Sci U S A. 2000; 97:3608–3613. [PubMed: 10725392]
51. Martinek S, Inonog S, Manoukian AS, Young MW. A role for the segment polarity gene *shaggy/GSK-3* in the *Drosophila* circadian clock. Cell. 2001; 105:769–779. [PubMed: 11440719]
52. Plautz JD, Kaneko M, Hall JC, Kay SA. Independent photoreceptive circadian clocks throughout *Drosophila*. Science. 1997; 278:1632–1635. [PubMed: 9374465]
53. Calleja M, Moreno E, Pelaz S, Morata G. Visualization of gene expression in living adult *Drosophila*. Science. 1996; 274:252–255. [PubMed: 8824191]
54. Lin DM, Goodman CS. Ectopic and increased expression of Fasciclin II alters motoneuron growth cone guidance. Neuron. 1994; 13:507–523. [PubMed: 7917288]
55. Dietzl G, Chen D, Schnorrer F, Su KC, Barinova Y, Fellner M, Gasser B, Kinsey K, Oppel S, Scheiblauer S, Couto A, Marra V, Keleman K, Dickson BJ. A genome-wide transgenic RNAi library for conditional gene inactivation in *Drosophila*. Nature. 2007; 448:151–156. [PubMed: 17625558]
56. Pfeiffer BD, Ngo TT, Hibbard KL, Murphy C, Jenett A, Truman JW, Rubin GM. Refinement of tools for targeted gene expression in *Drosophila*. Genetics. 2010; 186:735–755. [PubMed: 20697123]
57. Zhang L, Chung BY, Lear BC, Kilman VL, Liu Y, Mahesh G, Meissner RA, Hardin PE, Allada R. $DN1_p$ circadian neurons coordinate acute light and PDF inputs to produce robust daily behavior in *Drosophila*. Curr Biol. 2010; 20:591–599. [PubMed: 20362452]
58. Siegmund T, Korge G. Innervation of the ring gland of *Drosophila melanogaster*. J Comp Neurol. 2001; 431:481–491. [PubMed: 11223816]
59. Grima B, Chelot E, Xia R, Rouyer F. Morning and evening peaks of activity rely on different clock neurons of the *Drosophila* brain. Nature. 2004; 431:869–873. [PubMed: 15483616]
60. Yao Z, Macara AM, Lelito KR, Minosyan TY, Shafer OT. Analysis of functional neuronal connectivity in the *Drosophila* brain. J Neurophysiol. 2012; 108:684–696. [PubMed: 22539819]

61. Konopka RJ, Benzer S. Clock mutants of *Drosophila melanogaster*. Proc Natl Acad Sci U S A. 1971; 68:2112–2116. [PubMed: 5002428]

62. Wang JW, Beck ES, McCabe BD. A modular toolset for recombination transgenesis and neurogenetic analysis of *Drosophila*. PLoS One. 2012; 7:e42102. [PubMed: 22848718]

63. Jenett A, Rubin GM, Ngo TT, Shepherd D, Murphy C, Dionne H, Pfeiffer BD, Cavallaro A, Hall D, Jeter J, Iyer N, Fetter D, Hausenfluck JH, Peng H, Trautman ET, Svirskas RR, Myers EW, Iwinski ZR, Aso Y, DePasquale GM, Enos A, Hulamm P, Lam SC, Li HH, Laverty TR, Long F, Qu L, Murphy SD, Rokicki K, Safford T, Shaw K, Simpson JH, Sowell A, Tae S, Yu Y, Zugates CT. A GAL4-driver line resource for *Drosophila* neurobiology. Cell Rep. 2012; 2:991–1001. [PubMed: 23063364]

64. Rideout EJ, Dornan AJ, Neville MC, Eadie S, Goodwin SF. Control of sexual differentiation and behavior by the *doublesex* gene in *Drosophila melanogaster*. Nat Neurosci. 2010; 13:458–466. [PubMed: 20305646]

65. Collins B, Kaplan HS, Cavey M, Lelito KR, Bahle AH, Zhu Z, Macara AM, Roman G, Shafer OT, Blau J. Differentially timed extracellular signals synchronize pacemaker neuron clocks. PLoS Biol. 2014; 12:e1001959. [PubMed: 25268747]

66. Cyran SA, Yiannoulos G, Buchsbaum AM, Saez L, Young MW, Blau J. The Double-time protein kinase regulates the subcellular localization of the *Drosophila* clock protein Period. J Neurosci. 2005; 25:5430–5437. [PubMed: 15930393]

67. Ruben M, Drapeau MD, Mizrak D, Blau J. A mechanism for circadian control of pacemaker neuron excitability. J Biol Rhythms. 2012; 27:353–364. [PubMed: 23010658]

68. Stewart BA, Atwood HL, Renger JJ, Wang J, Wu CF. Improved stability of *Drosophila* larval neuromuscular preparations in haemolymph-like physiological solutions. J Comp Physiol A. 1994; 175:179–191. [PubMed: 8071894]

69. McCarthy EV, Wu Y, Decarvalho T, Brandt C, Cao G, Nitabach MN. Synchronized bilateral synaptic inputs to *Drosophila melanogaster* neuropeptidergic rest/arousal neurons. J Neurosci. 2011; 31:8181–8193. [PubMed: 21632940]

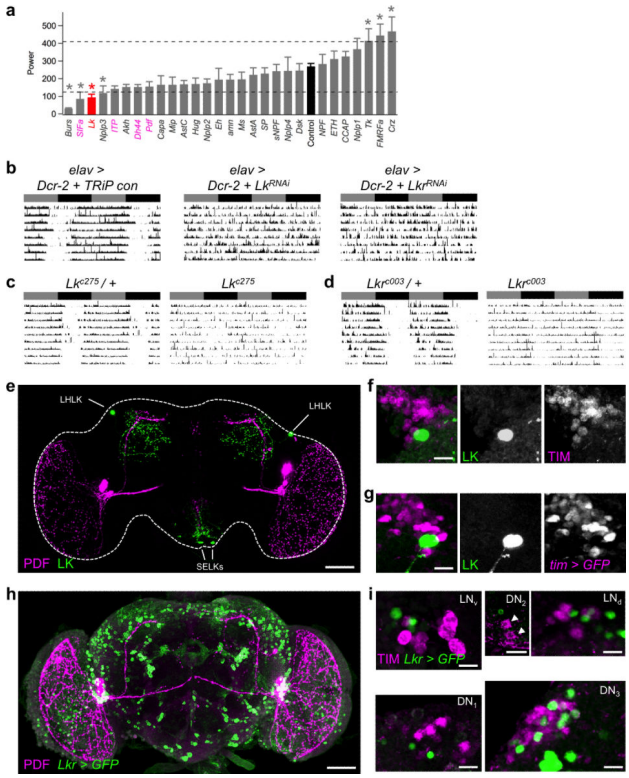

Figure 1. *Lk* and *Lkr* mutant circadian phenotypes and location of LK and LK-R expressing neurons

(**a**) Average rhythm strength (power) ± SEM of *UAS-RNAi* lines targeting neuropeptides driven pan-neuronally with *elav-Gal4.* Control: *elav > Dcr-2* + TRiP injection stock. Genes previously implicated in circadian rhythms or sleep are highlighted in pink, *Lk* in red. Dashed lines: control average ± 1 standard deviation, asterisks: power > 1 standard deviation different from control. (**b-d**) Representative actograms correspond to the average power of *Lk* and *Lkr* mutant flies for 10 days in DD after 3 days entrainment to 12:12 LD cycles (grey/black bars: subjective day/night). (**b**) RNAi knockdown of *Lk* and *Lkr.* (**c-d**) Lk^{c275} and Lkr^{c003} classical alleles compared to heterozygous controls. See **Supplementary Tables 1 and 2** for details and sample sizes. (**e**) LK is expressed in sub-oesophageal LK (SELKs) and Lateral Horn LK neurons (LHLKs), which arborize very close to s-LN_v dorsal projections (PDF staining). Dorsal up, ventral down here and in subsequent figures. (**f-g**) LHLK neurons are not clock neurons since they do not express TIM (**f**) or *tim-Gal4 > nlsGFP* (**g**). (**h**) LK-R neurons (*Lkr-Gal4 > nlsGFP*) are widely distributed in the central brain and (**i**) are not clock neurons: no TIM expression in the LN_v region, DN_1, DN_2 (arrowheads), LN_d or DN_3. Scale bars: 20μm, except 100μm in **e** and **h**. >8 brains examined for each anatomical observation. (See also **Supplementary Fig. 1-2**).

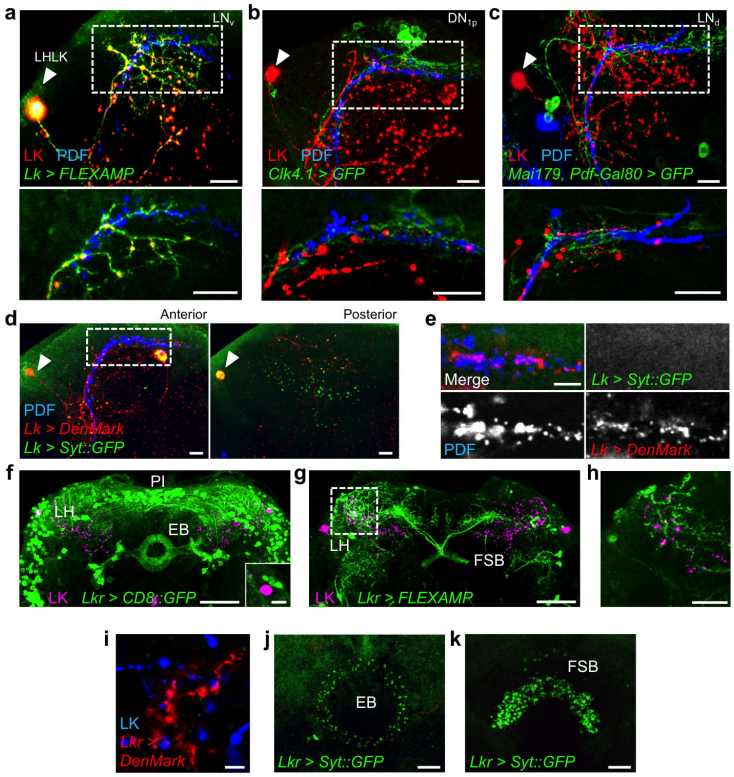

Figure 2. The anatomy of LHLK/LK-R neurons suggests they lie downstream of clock neurons

(**a-e**) White arrowheads indicate LHLK cell bodies. (**a-c**) Upper panels are z-projections, lower panels are single confocal sections of the regions indicated by white dashed rectangles in upper panels. LHLKs project close to (**a**) s-LN_vs (PDF staining), (**b**) DN_{1p}s (*Clk4.1-Gal4 > CD8::GFP*) and (**c**) LN_ds (*Mai179-Gal4; Pdf-Gal80 > CD8::GFP*). (**d**) LHLK dendrites (*Lk > DenMark*) and s-LN_v projections (PDF) are found in similar planes (anterior brain sections, left), whereas LHLK axon terminals (*Lk > Syt::GFP*) are enriched in more posterior sections (right). (**e**) Single confocal section of dashed rectangle in **d** shows that LHLK dendrites intermingle with s-LN_v dorsal projections. (**f**) *Lkr-Gal4 > CD8::GFP* labels neurons in the Lateral Horn (LH), Ellipsoid Body (EB) and Pars Intercerebrallis (PI). Inset: *Lkr-Gal4* is not expressed in LHLK neurons (single confocal section). (**g**) *Lkr > FLEXAMP* clone labels LK-R neurons in the LH projecting to the Fan-Shaped Body (FSB). (**h**) Single confocal section of the dashed square in **g** showing overlap of LK-R projections and LHLK arborizations and several potential contacts. (**i**) LHLK processes are close to LK-R dendrites (*Lkr > DenMark*, single confocal section). (**j-k**) LK-R outputs (Syt::GFP) are found predominantly in the EB (**j**) and FSB (**k**). Scale bars: 20μm, except 100μm in **f** and **g**. >8 brains examined for each anatomical observation. (See also **Supplementary Fig. 3**).

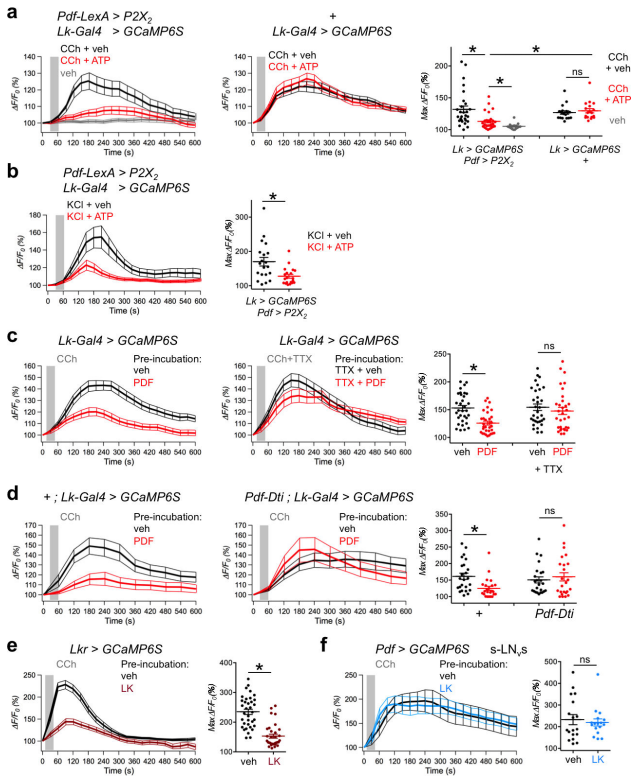

Figure 3. LHLK neurons are downstream of LN_vs

Mean GCaMP6S fluorescence (thick lines) normalized to initial level (vertical lines: SEM). Grey rectangles: timing of drug perfusion. Dot plots: distribution of Maximum $\Delta F/F_0$, horizontal line shows average ± SEM. Asterisks: significant difference by Kolmogorov-Smirnov (KS) test ($p<0.05$), ns: no significant difference. Sample sizes: n=x;y, where x is the number of neurons in y brains, from ≥2 independent experiments. (**a, left**) LHLK neuron responses to 10μM Carbachol (CCh + veh, n=28;8) are reduced by simultaneously activating LN_vs with 2.5 mM ATP (CCh + ATP, n=28;7, p=0.0003, D=0.536), but are still different from no CCh (veh, n=16;4, p=0.032, D=0.428). (**a, right**) Inhibition is lost in the absence of *Pdf-LexA > P2X2* expression (p=0.425, D=0.278, n=18;9 each). ATP significantly decreases LHLK responses in brains with *P2X2* vs without *P2X2* (p<0.0001, D=0.786). (**b**) LN_v activation also inhibits LHLK response to 35 mM KCl (KCl + ATP) compared to control (KCl + veh, p=0.008, D=0.5, n=20,10 each). (**c, left**) 20min pre-incubation with 100 μM PDF inhibits LHLK response to 10 μM CCh (p=0.0004, D=0.5, n=32;16 each). **(c, middle)** PDF inhibition of LHLKs is largely eliminated by 2 μM Tetrodotoxin (TTX) pre-incubation (p=0.232, D=0.25, n=32;16 each). (**d**) PDF inhibition of LHLKs (**left**, p=0.0082, D=0.458) is lost in *Pdf-Dti* brains (**right**, p=0.621, D=0.208, n=24,12 each). (**e**) LK-R neuron response to 100 μM CCh (n=33;4) is inhibited by 10min 100 μM LK pre-incubation (n=33;5, p<0.0001, D=0.675). (**f**) s-LN_v responses to 100 μM CCh (n=18;6) are not changed by pre-incubation with 100 μM LK (n=17;7, p=0.262, D=0.323). (See also **Supplementary Fig. 4**).

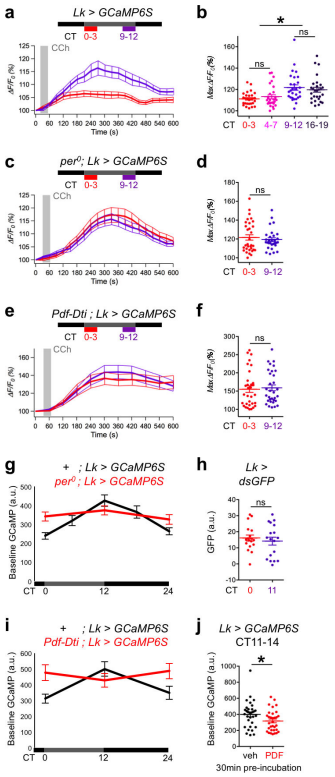

Figure 4. LHLK neuronal activity is rhythmically regulated by clock neurons

(**a-f**) LHLK responses to 10 μM CCh on day 1 in DD during 3hr time windows indicated above the line graphs by colored bars; dark grey and black bars show DD cycles. n=28;14 for each sample in **a-d**, n=32;16 for **e-f**, taken from ≥2 independent experiments. (**a**) LHLK excitability is rhythmic in wild type brains (p=0.0029, D=0.464, KS test). (**b**) Quantification of **a** and additional statistics: CT0-3 vs CT4-7 p=0.917, D=0.143; CT9-12 vs CT16-19 p=0.917, D=0.143; CT4-7 vs CT9-12 p=0.0029, D=0.464; CT4-7 vs CT16-19 p=0.0077, D=0.428; CT0-3 vs CT16-19 p=0.0029, D=0.464. LHLK excitability is not rhythmic in *per*^{0} mutants (**c-d**, p=0.987, D=0.125) or *Pdf-Dti* brains (**e-f,** p=0.383, D=0.219). (**g**) Baseline GCaMP6S intensity per LHLK cell body in brains from 1hr time windows on day 1 in DD (n=32;16 for each data point, grey/black bars show DD cycle, error bar: SEM). Baseline GCaMP6S levels are rhythmic in wild type brains (p<0.0001, H=28.69, 4d.f. by Kruskal-Wallis one-way ANOVA) but not in *per*^{0} mutants (p=0.2746, H=2.585, 2d.f.). (**h**) No rhythms are observed with *Lk-Gal4* expressing destabilized GFP (p=0.425, D=0.2778 by KS test, n=16;8 each). (**i**) The LHLK GCaMP6S rhythm (p=0.0005, H=15.41, 2d.f., Kruskal-Wallis ANOVA) is lost in brains lacking LN_vs (*Pdf-Dti,* p=0.6386, H=0.897, 2d.f., n=32;16 for each data point). (**j**) PDF treatment (100μM 30min pre-incubation before imaging) reduces baseline LHLK GCaMP6S levels during their peak phase (CT11-14; p=0.0343, D=0.344 by KS test, n=32;16 each).

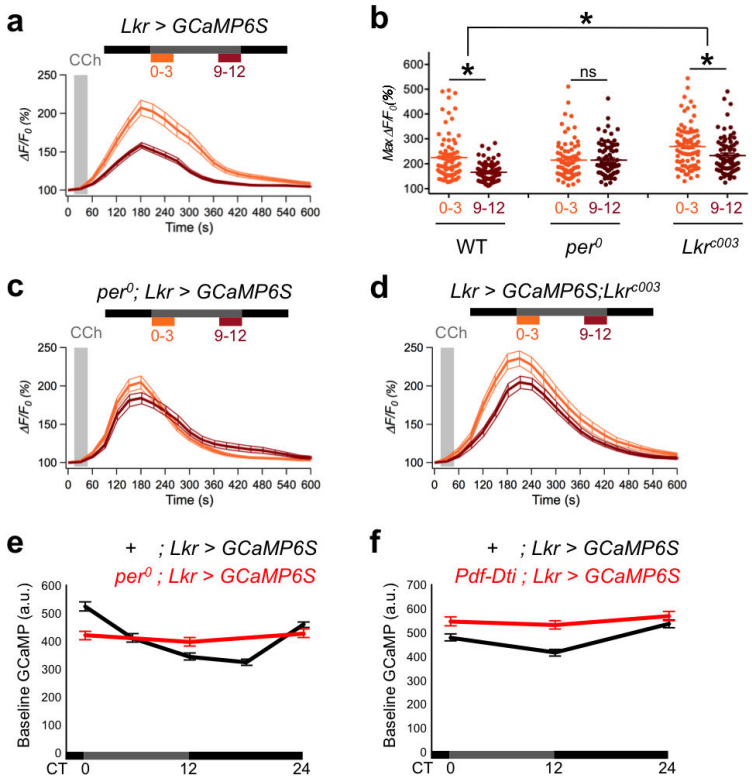

Figure 5. LHLK activity rhythms propagate to LK-R neurons

Only LK-R neurons with cell bodies in the lateral horn were imaged. Excitability (**a-d**) and neuronal activity (**e-f**) measurements and statistics as in **Fig. 4**. Data are from ≥2 independent experiments. (**a**) Lateral horn LK-R neuron excitability (response to 100 μM CCh) is rhythmic (n=80;10 for each sample, p<0.0001, D=0.375). (**b**) Quantification of **a,c-d**. (**c**) The rhythm is lost in *per*^{0} mutants (n=80;10 each, p=0.798, D=0.1) and (**d**) dampened in *Lkr*^{c003} hypomorphs, although still significant (n=80;10 each, p=0.0036, D=0.275). LK-R excitability is significantly higher in *Lkr*^{c003} mutants compared to wild type in both time windows (CT0-3 p=0.0001, D=0.337, CT9-12 p<0.0001, D=0.512) (**e**) Lateral horn LK-R baseline GCaMP6S levels are rhythmic in wild type brains (p<0.0001, H=200, 4d.f.; CT0 n=290;12, CT5 n=290;12, CT11 n=255;12, CT17 n=308;12, CT23 n=289;12). This rhythm is lost in *per*^{0} mutants (p=0.2918, H=2.463, 2d.f.; CT0 n=315;12, CT11 n=294;12, CT23 n=316;12) and in (**f**) brains lacking LN_vS (*Pdf-Dti*, p=0.6759, H=0.7834, 2d.f.; CT0 n=277;10, CT11 n=267;10, CT23 n=273;10) compared to controls (p<0.0001, H=33.72, 2d.f.; CT0 n=234;10, CT11 n=273;10, CT23 n=267;10).

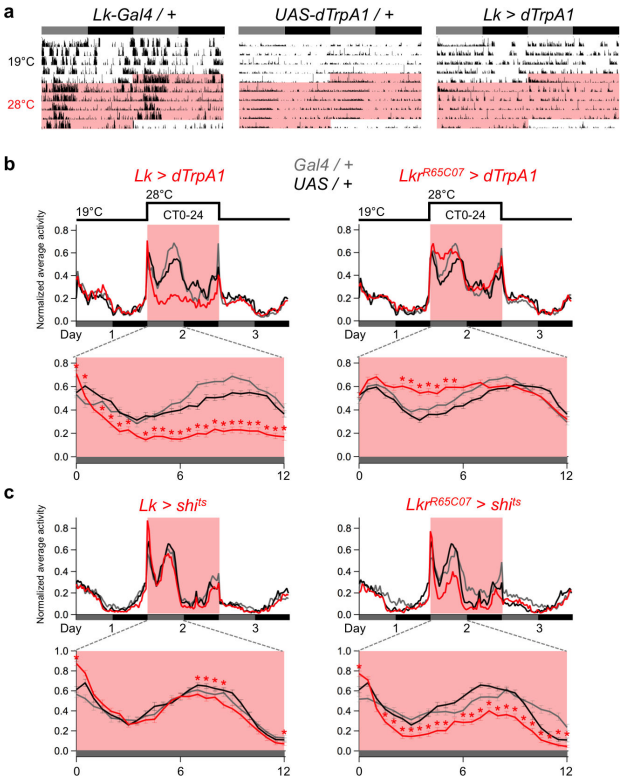

Figure 6. LK and LK-R neuron signaling controls locomotor activity levels

(**a**) Representative actograms of flies maintained 6 days in DD at 19°C and then 5 days at 28°C (red shaded area). Grey and black bars: subjective day and night. Rhythms of control flies (*Lk-Gal4 / +* and *UAS-dTrpA1 / +*) become stronger at 28°C compared to 19°C but become weaker when activating LK neurons with dTrpA1 at 28°C (*Lk > dTrpA1*). See **Supplementary Table 2** for details and for LK-R and DH44 neuron activation data. (**b-c**) Acute (24hr, red shaded area) activation (**b**) and inhibition (**c**) of LK and LK-R neurons. Graphs show the population average locomotor activity over 3 days in DD, with the first 12hr of activation magnified in insets below (error bars: SEM). Asterisks: significant differences between experimental flies and both parental controls ($p<0.05$ by KS test). (**b, left**) LK neuron activation decreased locomotor activity while (**b, right**) LK-R^{R65C07} neuron activation increased locomotor activity during the first 6hr. Locomotor activity recovered to normal levels on day 3 in both experiments. Sample sizes: *Lk-Gal4/+* n=62; *dTrpA1/+* n=62; *Lk>dTrpA1* n=63; *Lkr^{R65C07}-Gal4/+* n=94; *dTrpA1/+* n=94; *Lkr^{R65C07}>dTrpA1* n=93. Data are from 2 (left) or 3 (right) independent experiments. (**c, left**) Inhibiting synaptic transmission from LK neurons had minimal effects on locomotor activity, while (**c, right**) inhibiting LK-R^{R65C07} neurons reduced locomotor activity through most of the subjective day. Sample sizes: *Lk-Gal4/+* n=63; *shi^{ts}/+* n=62; *Lk>shi^{ts}* n=63; *Lkr^{R65C07}-Gal4/+* n=62; *Lkr^{R65C07}>shi^{ts}* n=62. Data are from 2 independent experiments. (See also **Supplementary Fig. 5-6**).

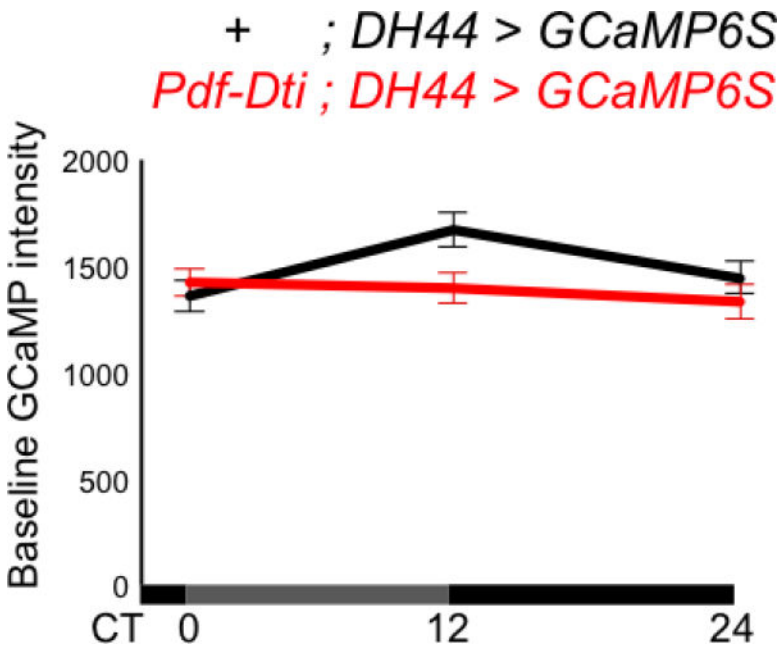

Figure 7. Clock electrical rhythms propagate through multiple output circuits

Baseline GCaMP6S levels oscillate in DH44 neurons (p=0.0033, H=11.45, 2d.f.; CT0 n=115;23, CT11 n=125;23, CT23 n=124;23). This rhythm is lost in brains lacking LN_vs (*Pdf-Dti*, p=0.2585, H=2.705, 2d.f.; CT0 n=103;19, CT11 n=96;19, CT23 n=100;19). Statistics as in **Fig. 4-5**. Data are from 3 independent experiments.